THE ASTROPHYSICAL JOURNAL, 470:L85–L88, 1996 October 20

INFRARED SPECTROSCOPY OF THE GRAVITATIONALLY LENSED QUASAR B1422+231: Mg II λ2798 AND Fe II EMISSION FROM THE BROAD-LINE GAS AT $z = 3.62$

KIMIAKI KAWARA,[1,2,3] TAKASHI MURAYAMA,[3,4] YOSHIAKI TANIGUCHI,[3,4,5] AND NOBUO ARIMOTO[6]

Received 1996 June 26; accepted 1996 August 7

ABSTRACT

The rest-frame UV-optical (2000–5300 Å) spectrum of the gravitationally lensed flat-spectrum radio-loud quasar B1422+231 system at $z = 3.62$ is presented. The spectrum is similar to the Large Bright Quasar Survey (LBQS) composite spectrum (Francis et al.), which indicates no significant UV-optical spectral evolution in some quasars at $0 < z < 3.6$. The Fe II(UV + optical)/Mg II λ2798 flux ratio is 12.2 ± 3.9, which is comparable to 8.9 for the LBQS composite spectrum of quasars at $z = 1$–2 analyzed in this work, and 7.8 ± 2.6 for quasars at $z = 0.15$–0.63 analyzed by Wills, Netzer, & Wills. It is concluded that the majority of stars in the host galaxy of B1422+231 have formed much earlier (~1.5 Gyr) than $z = 3.6$. The first detection of [O III] λ5007 in a quasar beyond $z = 3$ is also reported.

Subject headings: cosmology: observations — galaxies: evolution — galaxies: formation — gravitational lensing — quasars: emission lines — quasars: individual (B1422+231)

1. INTRODUCTION

The large luminosities of quasars provide a powerful tool for studying the properties of the universe, including the major epoch of galaxy formation and the current value of the Hubble time. The broad emission line ratios, in particular the ratio of the Fe II/Mg II λ2798 emission lines, can be used as a cosmic clock to measure the age of quasar host galaxies, if the Fe/Mg abundance can be derived from supernova nucleosynthesis prescriptions (Wheeler, Sneden, & Truran 1989; Hamann & Ferland 1993). We present infrared spectroscopy for measuring the Mg II λ2798 and Fe II emission of the flat-spectrum radio source system B1422+231 that was identified with a quasar at $z = 3.62$ by Patnaik et al. (1992). B1422+231, with the total magnitude $r = 15.6$ mag (Yee & Bechtold 1996), is one of the lensed systems with the brightest apparent luminosity, comprising four components with a maximum separation of 1.″3 (Patnaik et al. 1992; Lawrence et al. 1992).

2. OBSERVATIONS AND REDUCTIONS

B1422+231 was observed using the long-slit CRSP (CRyogenic SPectrometer; Joyce 1995) with a 256 × 256 InSb detector array at the f/15 focus of the Kitt Peak National Observatory (KPNO) 4 m telescope on 1995 May 14. A 1.″44 × 49″ slit with a scale of 0.″36 pixel^{-1} was placed on the intensity peak of the object in the east-west direction. A 200 line mm^{-1} grating with a blaze angle of 17.°5 was used in third order at I (0.94–1.1 μm), in second order at J (1.095–1.349 μm) and H (1.500–1.788 μm), and in first order at K (2.055–2.430 μm). OH airglow lines and HeNeAr lamp spectra were used to calibrate the wavelength scale and to measure the spectral resolution. The accuracy of the wavelength scale calibration is 70 km s^{-1} at I, 130 km s^{-1} at J, 130 km s^{-1} at H, and 110 km s^{-1} at K. The typical FWHMs of the spectral resolution are 1100 km s^{-1} at I, 1300 km s^{-1} at J, 1000 km s^{-1} at H, and 1500 km s^{-1} at K.

The object was observed by being shifted along the slit by 10″ between exposures. Each exposure time was 300 s at all the bands except for K, where a 50 s exposure was used to avoid saturation by the background radiation. The total integration times per band were 1500 s for I, J, and H, and 1000 s for K. The residual sky emission was removed by fitting the sky emission on the adjacent sky pixels.

A faint standard star HD 106965 (A2, $K = 7.315$) was used to calibrate the flux scale and correct for telluric extinction. A 9000 K blackbody spectrum that fits to the *JHKL* magnitudes (Elias et al. 1982) within 1.2% deviation was used for flux scale calibration. The I-band fluxes, for which no photometric magnitudes have been published, were derived by assuming this blackbody spectrum; the accuracy in the I-band fluxes was estimated to be 5% or better. The flux of the zero-magnitude star is given by Leggett et al. (1996).

The VLA map (Patnaik et al. 1992) indicates that some light from the object must have been out of the slit due to seeing. The FWHMs of the one-dimensional seeing profiles of the object varied with time from band to band in a range of 1.″4–2.″1, causing variations in light to fall into the 1.″44 slit; light received by the array decreased down to 30% of the value under 1.″4 seeing. The effect of temporal variations in seeing was corrected by using the successive exposures of the object. The correlation between the signal and the seeing size (FWHM) in each band was applied to the object data in that

[1] The Institute of Space and Astronautical Science, 3-1-1, Yoshinodai, Sagamihara-shi, Kanagawa 229, Japan.
[2] Present address: ISO Science Operations Centre, Astrophysics Division of ESA, Villafranca, 28080 Madrid, Spain; kkawara@iso.vilspa.esa.es.
[3] Visiting Astronomer, Kitt Peak National Observatory, National Optical Astronomy Observatories, which are operated by the Association of Universities for Research in Astronomy, Inc., under contract with the National Science Foundation.
[4] Astronomical Institute, Tohoku University, Aoba, Sendai, 980-77, Japan; murayama@astroa.astr.tohoku.ac.jp, tani@astroa.astr.tohoku.ac.jp.
[5] Royal Greenwich Observatory, Madingly Road, Cambridge CB3 0EZ, England, UK.
[6] Institute of Astronomy, University of Tokyo, 2-21-1, Osawa, Mitaka, Tokyo 181, Japan; arimoto@mtk.ioa.s.u-tokyo.ac.jp.

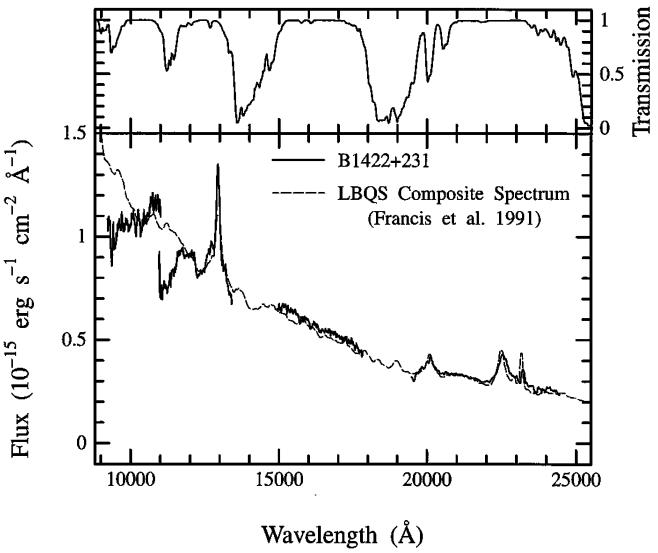

FIG. 1.—The bottom panel shows the spectrum of B1422+231 at $z = 3.62$ in the observed frame with the LBQS composite spectrum superimposed. The top panel shows the atmospheric transmission curve at the Kitt Peak (Manduca & Bell 1979).

band in order to normalize the signals to those under seeing of 1.″4. The standard was measured under seeing of 1.″4. The object and the standard were taken at similar zenith distance, and the zenith distance of the object was bracketed by those of the standard. The flux of the object was adjusted to be brighter by a factor of 1.1 in order to account for the difference in the amount of missed light due to seeing between the extented (object) and the point (standard) sources. The photometric accuracy in 0.94–0.98 μm, in 1.11–1.15 μm, longward of 1.325 μm in the J band, and shortward of 1.965 μm in the K band is largely uncertain, due to the time variation in strength of the H_2O absorption bands (see the top panel in Fig. 1). The accuracy in 2.00–2.03 μm is also uncertain, due to the CO_2 absorption bands. For the other wavelengths, the accuracy of absolute photometry is limited by the seeing variations and is estimated to be around 10%. The accuracy of the relative photometry among the four bands is much better than this value, so that the overall slope of the resultant 0.94–2.43 μm spectrum should be accurate enough for the purpose of this work.

3. RESULTS AND ANALYSIS

Figure 1 shows the 0.94–2.43 μm spectrum of B1422+231 on the bottom panel and the atmospheric transmission curve on the top (Manduca & Bell 1979). The composite spectrum of quasars in the Large Bright Quasar Survey (LBQS), which is the average spectrum of ~700 quasars at $z = 1$–2 (Francis et al. 1991), is superimposed for comparison. There is a striking similarity in continua and line features between B1422+231 and the LBQS composite spectrum. In the regions where the atmospheric transmission is low due to H_2O absorption bands, the B1422+231 continuum is consistently lower than that of the LBQS composite spectrum. These deviations are probably due to incomplete correction for telluric absorption. In the rest of this Letter, we will ignore the region between 1.10 and 1.16 μm where the telluric H_2O absorption is the strongest. Combining this similarity with the fact that there is no evidence for redshift-dependent spectral changes in 1000–2200 Å in quasars of the same luminosity at $z < 3.8$ (Osmer, Porter, & Green 1994), we see that our results would extend their claim to 5200 Å on cosmological timescales up to $z = 3.6$.

Figure 1 shows the emission lines Mg II λ2798, H_γ, Hβ, and [O III] λ5007 as well as a marginal detection of C III] λ2326. Note that this is the first detection of [O III] λ5007 in a quasar beyond $z = 3$. Relative to Hβ, [O III] λ5007 is smaller in B1422+231 than in the LBQS composite. This may simply be due to the luminosity effect; [O III]/Hβ decreases with increasing Hβ luminosity (Steiner 1981). In fact, the mean absolute B magnitude of LBQS quasars is $M_B \sim -23.3$ for $q_0 = 0.0$ and $H_0 = 75$ km s^{-1} Mpc^{-1}, while the total magnitude, $r = 15.6$ mag (Yee & Bechtold 1996), of the B1422+231 system implies $M_B \sim -28.2$ mag for the source, in the absence of the lens after correction for a total magnification factor of 15–30 (Hogg & Blandford 1994; Kormann, Schneider, & Bartelmann 1994), although this magnitude must be uncertain at least 1 mag, from the uncertainty in the lensing.

The broad feature of optical Fe II emission lines is present at 2.05–2.2 μm. The feature shortward of the Mg II λ2798 emission line is due to UV Fe II emission lines, which is evidenced by the dip near 1.25 μm or 2700 Å in the rest frame. The theoretical models of Fe II and H I emission predict that the major part of UV Fe II emission lies 2000–3000 Å in the rest frame or 0.92–1.38 μm in the observed frame, and Balmer continuum emission contributes a significant fraction of the spectrum between 2700 and 3800 Å, or 1.24 and 1.75 μm (Wills, Netzer, & Wills 1985).

Figure 2 shows the rest-frame spectrum of B1422+231 with the power law subtracted and with the best-fit synthetic spectrum comprised of Fe II and Balmer continuum emission and other broad lines. The continuum level on the short-wavelength side was fixed to the total flux of the system between 1330 and 1380 Å, which was obtained from observations taken by Impey et al. (1996) 1 month before our observations. The level on the long-wavelength side was chosen by fitting the power-law continuum and the Fe II template simultaneously, to minimize the residual between 4450 and 4750 Å and beyond 5100 Å. We used the Balmer continuum template that was generated to approximate the emission-line strengths seen in 0742+318 (see Fig. 3*d* of Wills et al. 1985). The Fe II emission profile of the unusually strong Fe II–emitting low-ionization BAL quasar PG 0043+039 (Turnshek et al. 1994) was used as the Fe II template. Due to the poor fitting over the entire wavelength range by the single template, two Fe II templates were used: one for shortward of 3000 Å and the other for longward of 3000 Å. The excess emission around 2300 Å may be caused by the C III] λ2326 line.

Table 1 summarizes the strengths of the emission features and compares them with those of the LBQS composite spectrum to which the same analysis used for B1422+231 was applied. Note that the uncertainties in Table 1 include the 1 σ standard deviations of the fitting residuals and the 1 σ standard deviations from the 10% photometric accuracy. The flux ratio Fe II(UV + optical)/Mg II of B1422+231 is comparable to that of the LBQS composite spectrum: 12.2 ± 3.9 for B1422+231 and 8.9 for the LBQS composite. Note that Fe II(UV) and denote Fe II(optical) denote Fe II emission in 2000–3000 Å and 3500–6000 Å, respectively, in the rest frame. The analysis of eight quasars (Wills et al. 1985) indicated a mean ratio of 7.8 ± 2.6 for low redshifts at

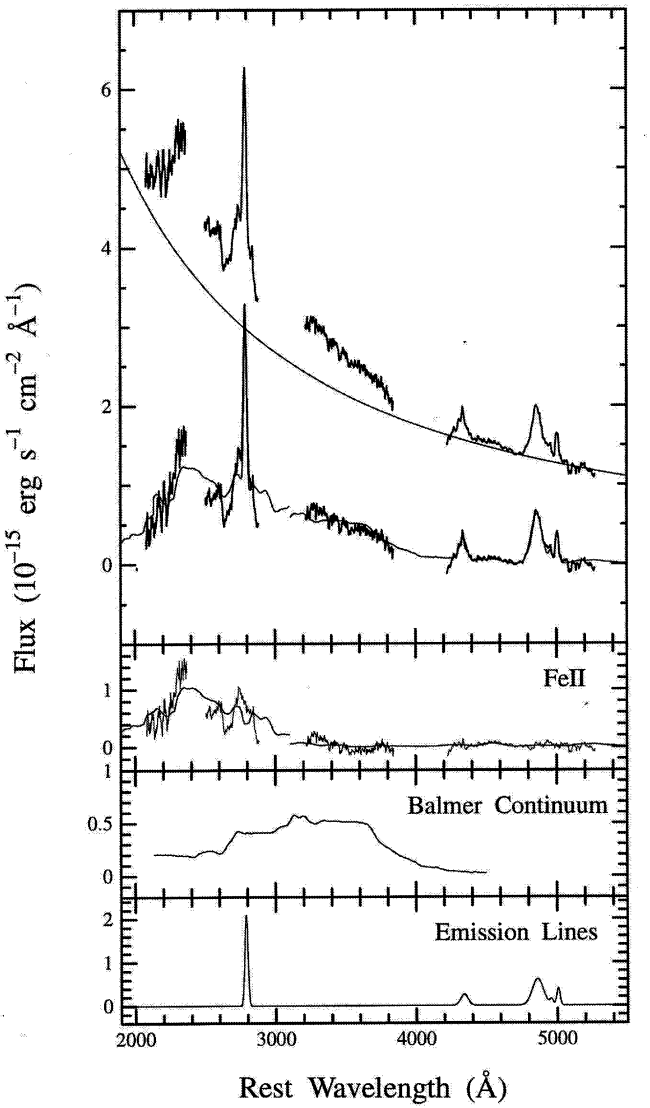

FIG. 2.—The upper panel gives the rest-frame spectrum of B1422+231 and the same spectrum with the power-law continuum subtracted, together with the power-law continuum and the synthetic spectrum comprised of the Fe II and Balmer continuum emission and other emission lines. Note that the rest-frame spectrum was derived by dividing the observed frame spectrum by $(1 + z)$ after converting observed wavelengths into the rest-frame wavelengths. The spectrum shown in the second panel is the extracted Fe II emission of B1422+231, together with the best-fitted Fe II template. The third and fourth panels show the best-fitted templates of the Balmer continuum and other emission lines, respectively.

$z = 0.15–0.63$. The effect of luminosity can be checked by a comparison with 3C 273 ($M_B \sim -27.3$), whose luminosities from the UV to radio are comparable to those of the source quasar of B1422+231 (Chini et al. 1989; Kühr et al. 1981; Patnaik et al. 1992). The ratio is 10.6 ± 1.4 in 3C 273 (Wills et al. 1985), so there are no significant differences in Fe II/Mg II between 3C 273 and B1422+231. Hence, B1422+231 shows no evolution in Fe II/Mg II on cosmological timescales up to $z = 3.6$. The radio properties do not alter this conclusion, because B1422+231 and 3C 273 are core-dominant flat-spectrum radio sources. It is noted that the LBQS is a predominantly radio-quiet sample.

4. DISCUSSION

Hill, Thompson, & Elston (1993) have used the rest-frame optical spectra of four bright quasars at $z \sim 2.5$ (one radio-quiet, one radio-loud, and two BAL quasars) to argue that optical Fe II emission at high redshift is strong compared with the emission from low-redshift quasars. Elston, Thompson, & Hill (1994) have found strong optical Fe II emission in two flat-spectrum radio-loud quasars at $z \sim 3.3$ and compared the Fe II enrichment timescales with the age of the universe. There is, however, a drastic variation in the strength of the optical Fe II emission from quasar to quasar. The total Fe II emission is usually dominated by the UV Fe II emission: the ratio of the UV Fe II to optical Fe II emission ranges from 4 to 12. Most importantly, all quasars have strong UV Fe II emission, regardless of the strength of their optical Fe II. Thus, the UV Fe II emission offers a better indicator for Fe abundance (Wills et al. 1985). Because the Mg^+ and Fe^+ zones are almost the same (the ionization potentials of Fe^0 and Fe^+ are very close to the counterparts of Mg), Fe II/Mg II can be a good measure of the Fe/Mg abundance ratio in the broad-line gas if the excitation of the lines is known.

The most significant contribution of the present work is to provide the ratio Fe II/Mg II, including UV Fe II emission lines; the ratio in the broad-line gas of some quasars at $z = 3.6$ is almost identical to those at the low-redshift quasars. This may imply that the Fe/Mg abundance at the center of some quasar host galaxies did not change after $z = 3.6$. If standard stellar nucleosynthesis prescriptions are correct, both Mg and Fe should be synthesized in stars of host galaxies: Mg is preferentially produced in massive star supernovae (SNe II, Ib, and Ic) on short timescales (2–10 Myr), while Fe is created mainly by accreting white dwarf supernovae (SNe Ia) in much longer timescales (1–2 Gyr). The Fe/Mg abundance ratio should be 1/4–1/2 of the solar value until SNe Ia start to produce significant amount of Fe. When SNe Ia dominate the Fe production, the Fe/Mg abundance increases up to the values in low-redshift quasars and is then kept nearly constant. Although it is not straightforward to derive the Fe/Mg abundance from the present data, the similarity in Fe II/Mg II between B1422+231 and low-redshift quasars (and the LBQS composite spectrum) suggests that the host galaxy of B1422+231 had already been in the late-evolutionary phase of the Fe enrichment at $z = 3.6$. Yoshii, Tsujimoto, & Nomoto (1996) derived ~1.5 Gyr for the lifetime of SN Ia progenitors from the analysis of the O/Fe and Fe/H abundances in solar neighborhood stars. If the Fe enrichment started at 1.5 Gyr after the onset of the first star formation, the host galaxy of B1422+231 would have formed at $z \sim 9$ or earlier for $q_0 = 0.0$ and $H_0 = 75$ km s^{-1} Mpc^{-1}. The model with $q_0 = 0.5$ should have $H_0 \leq 30$ km s^{-1} Mpc^{-1} to be consistent with our results, but this is incompatible with the recent measurements of the Hubble constant (e.g., Kennicutt, Freedman, & Mould 1995).

We are grateful to the staff of KPNO, and particularly Dick Joyce for technical support and assistance with the observations. We would like to thank N. Trentham and the anonymous referee for a careful reading of the manuscript and useful comments, H. Shibai, M. Imanishi, and S. Okamura for useful suggestions on telluric absorption bands and the Hubble constant, and Y. Yoshii and T. Tsujimoto for providing a preprint on the lifetime of SN Ia progenitors. We acknowledge the use of IRAF, which is distributed by the National Optical

TABLE 1

MEASUREMENTS OF EMISSION FEATURES

TRANSITION	RELATIVE FLUX				B1422+231	
	B1422[a]	LBQS[b]	Low z[c]	3C 273[d]	EW[e]	FWHM[f]
Mg II λ2798	97.0 (5.8)	105	120	138	19.5	2500
[O II] λ3727	<3.6[g]	3.9	⋯	⋯	<1.1	⋯
H_γ + [O III] λ4363	27.9 (4.3)[h]	39.1	36	36	10.6	3900
Hβ	100 (7.0)	100	100	100	44.9	5500
[O III] λ5007	19.6 (2.1)	37.8	⋯	⋯	9.2	840
Fe II (UV: 2000–3000 Å)	1120 (347)	789	790	1175	⋯	⋯
Fe II (optical: 3500–6000 Å)	67.8 (22)	148	143	290	⋯	⋯
Balmer continuum	691 (117)	513	807	700	⋯	⋯

NOTES.—The total Hβ flux in B1422 = 5.96×10^{-14} ergs s^{-1} cm^{-2}. Power-law index of B1422, $\alpha = +0.54$, where $F_\nu \propto \nu^{-\alpha}$.

[a] Numbers in parentheses denote the uncertainties, which include the 1 σ standard deviations of the fitting residuals and the 1 σ standard deviations from the 10% photometric accuracy.

[b] The flux intensities were extracted from the spectrum by Francis et al. (1991) by applying the same analysis as used for B1422+231.

[c] Mean values of eight quasars at $z = 0.15–0.63$ (Wills et al. 1985).

[d] Mean values of 3C 273 extracted from two models (Wills et al. 1985).

[e] Rest-frame values in angstroms.

[f] FWHM after correction for the instrumental broadening in km s^{-1}.

[g] 3 σ upper limits assuming a FWHM of 1000 km s^{-1}.

[h] The real error may be significantly larger than the quoted value due to the deep CO_2 absorption. See Fig. 1.

Astronomy Observatories. This work was financially supported in part by Grant-in-Aids for the Scientific Research (Nos. 06640349, 07222206, and 0704405) of the Japanese Ministry of Education, Culture, Sport, and Science, and by the Foundation for Promotion of Astronomy, Japan. Y. T. would like to thank K. Tritton, R. Terlevich, E. Terlevich, and I. Salamanca for their warm hospitality at the Royal Greenwich Observatory.

REFERENCES

Chini, R., Biermann, P. L., Kreysa, E., & Gemünd, H.-P. 1989, A&A, 221, L3
Elias, J. H., Frogel, J. A., Matthews, K., & Neugebauer, G. 1982, AJ, 87, 1029
Elston, R., Thompson, K. L., & Hill, G. J. 1994 Nature, 367, 250
Francis, J. P., Hewett, P. C., Foltz, C. B., Chaffee, F. H., Weymann, R. J., & Morris, S. L. 1991, ApJ, 373, 465
Hamann, F., & Ferland, G. 1993, ApJ, 418, 11
Hill, G. J., Thompson, K. L., & Elston, R. 1993, ApJ, 414, L1
Hogg, D. W., & Blandford, R. D. 1994, MNRAS, 268, 889
Impey, C. D., Folts, C. B., Petry, C. E., Browne, I. W. A., & Patnaik, A. R. 1996, ApJ, 462, L53
Joyce, R. 1995, CRSP Operating Manual, Version 7 (Tucson: KPNO)
Kennicutt, R. C., Jr., Freedman, W. L., & Mould, J. M. 1995, AJ, 110, 1476
Kormann, R., Schneider, P., & Bartelmann, M. 1994, A&A, 286, 357
Kühr, H., Witzel, A., Pauliny-Toth, I. I. K., & Nauber, U. 1981, A&AS, 45, 367
Lawrence, C. R., Neugebauer, G., Weir, N., Matthews, K., & Patnaik, A. R. 1992, MNRAS, 259, 5P
Leggett, S. K., Allard, F., Berriman, G., Dahn, C. C., & Hauschildt, P. H. 1996, ApJS, 104, 117
Manduca, A., & Bell, B. A. 1979, PASP, 91, 848
Osmer, P. S., Porter, A. C., & Green, R. F. 1994, ApJ, 436, 678
Patnaik, A. R., Browne, I. W. A., Walsh, D., Chaffee, F. H., & Foltz, C. B. 1992, MNRAS, 259, 1P
Steiner, J. E. 1981, ApJ, 250, 469
Turnshek, D. A., et al. 1994, ApJ, 428, 93
Wheeler, J. C., Sneden, C., & Truran, J. W. 1989, ARA&A, 27, 279
Wills, B. J., Netzer, H., & Wills, D. 1985, ApJ, 288, 94
Yee, H. K. C., & Bechtold, J. 1996, AJ, 111, 1007
Yoshii, Y., Tsujimoto, T., & Nomoto, K. 1996, ApJ, 462, 266